

# Aggregation of the Salivary Proline-Rich Protein IB5 in the Presence of the Tannin EgCG

Francis Canon,<sup>†,‡</sup> Franck Paté,<sup>§</sup> Véronique Cheynier,<sup>§</sup> Pascale Sarni-Manchado,<sup>§</sup> Alexandre Giuliani,<sup>†,⊥</sup> Javier Pérez,<sup>||</sup> Dominique Durand,<sup>&</sup> Joaquim Li,<sup>#</sup> and Bernard Cabane<sup>\*,#</sup>

<sup>†</sup>DISCO beamline, Synchrotron Soleil, l'Orme des Merisiers, 91192 Gif sur Yvette, France

<sup>‡</sup>INRA, UMR1324 Centre des Sciences du Goût et de l'Alimentation, F-21000 Dijon, France

<sup>§</sup>INRA, UMR1083 Sciences pour l'Oenologie, F-34060 Montpellier, France

<sup>⊥</sup>UAR 1008, CEPIA, INRA, BP 71627, F-44316 Nantes, France

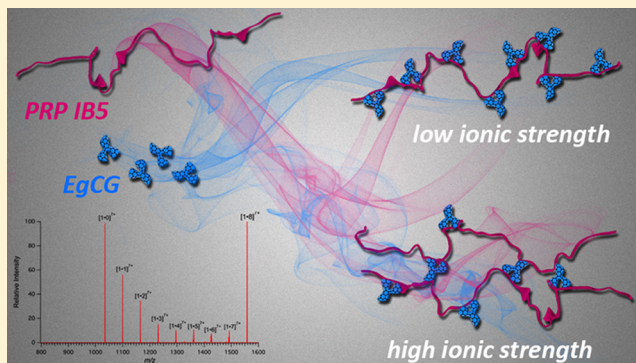
<sup>||</sup>SWING beamline, Synchrotron SOLEIL, BP 48, 91192 Gif-sur-Yvette, France

<sup>&</sup>IBBMC, CNRS UMR 8619, Université Paris-Sud, 91405 Orsay, France

<sup>#</sup>PMMH, CNRS UMR 7636, Université Pierre et Marie Curie, Université René Diderot, ESPCI, 10 rue Vauquelin, 75231 Paris cedex 05, France

## Supporting Information

**ABSTRACT:** In the mouth, proline-rich proteins (PRP), which are major components of stimulated saliva, interact with tannins contained in food. We report *in vitro* interactions of the tannin epigallocatechin gallate (EgCG), with a basic salivary PRP, IB5, studied through electrospray ionization mass spectrometry (ESI-MS), small-angle X-ray scattering (SAXS), and dynamic light scattering (DLS). In dilute protein (IB5) solutions of low ionic strength (1 mM), the proteins repel each other, and the tannins bind to nonaggregated proteins. ESI-MS experiments determine the populations of nonaggregated proteins that have bound various numbers of tannin molecules. These populations match approximately the Poisson distribution for binding to  $n = 8$  sites on the protein. MS/MS experiments confirm that complexes containing  $n = 1$  to 8 EgCG molecules are dissociated with the same energy. Assuming that the 8 sites are equivalent, we calculate a binding isotherm, with a binding free energy  $\Delta\mu = 7.26RT_a$  ( $K_d = 706 \mu\text{M}$ ). In protein solutions that are more concentrated (0.21 mM) and at higher ionic strength (50 mM, pH 5.5), the tannins can bridge the proteins together. DLS experiments measure the number of proteins per aggregate. This number rises rapidly when the EgCG concentration exceeds a threshold (0.2 mM EgCG for 0.21 mM of IB5). SAXS experiments indicate that the aggregates have a core–corona structure. The core contains proteins that have bound at least 3 tannins and the corona has proteins with fewer bound tannins. These aggregates coexist with nonaggregated proteins. Increasing the tannin concentration beyond the threshold causes the transfer of proteins to the aggregates and a fast rise of the number of proteins per aggregate. A poisoned growth model explains this fast rise. Very large cationic aggregates, containing up to 10 000 proteins, are formed at tannin concentrations (2 mM) slightly above the aggregation threshold (0.2 mM).



## INTRODUCTION

About 25% of all proteins in higher eukaryotic organisms are intrinsically disordered proteins (IDPs), i.e. they lack well-structured 3D conformation and do not form a compact globular structure but instead populate dynamic conformational ensembles.<sup>1–5</sup> This is a consequence of their peculiar sequences, which have sometimes a bias toward charged and polar amino acids and away from bulky hydrophobic residues, and often a low sequence complexity with repeated short amino acid sequences.<sup>6</sup> Despite their lack of a well-defined 3D conformation, IDPs perform a variety of essential functions that are related to their lack of ordered conformations.<sup>1–5</sup>

Salivary proline-rich proteins (PRPs), which constitute about two-thirds of proteins secreted by the human parotid gland, have this type of sequence signature.<sup>6–8</sup> Salivary PRPs are divided into acidic and basic types that contain repeated sequences with high proportions of Pro, Gly, and Glu or Gln residues, respectively.<sup>8–10</sup> Despite their structural similarities, they have different functions. While acidic PRPs also bind to hydroxyapatite, the only described function of basic PRPs is to

Received: October 21, 2012

Revised: January 6, 2013

Published: January 8, 2013

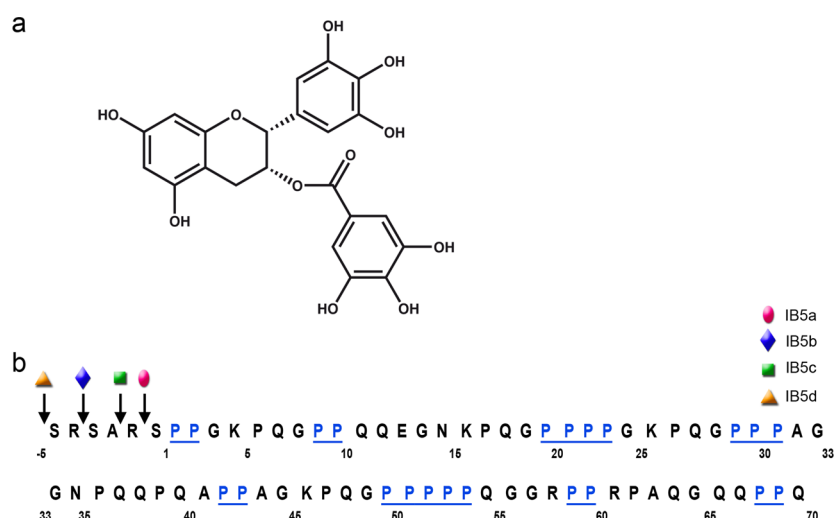


**Figure 1.** (a) Molecular structure of the tannin EgCG and (b) sequence of the salivary protein IB5.

bind tannins and protect the organism against their antinutritional effects.<sup>9,10</sup>

Tannins are phenolic compounds ubiquitous in plants and plant-derived products, known to reduce protein assimilation, because they bind digestive enzymes and dietary proteins.<sup>9–13</sup> The protective role of PRPs against dietary tannins may take place through either of two distinct mechanisms: (a) capture of tannins that thus become unable to inhibit digestive enzymes<sup>9–13</sup> and (b) astringency, a tactile perception in the mouth that signals an excessive concentration of tannins.<sup>13–21</sup> There is a debate regarding the mechanism of astringency.<sup>18,19</sup> The most generally accepted view is that it results from tannin aggregation with salivary proteins, causing a loss in the lubricating power of saliva.<sup>10,17,20–23</sup> An alternative hypothesis is that tannins act on receptors in the mucosa, like other primary tastes such as sourness or bitterness.<sup>24–26</sup> However, astringency increases upon repeated exposure, in contrast to taste sensations,<sup>20</sup> suggesting that it involves mechanical rather than chemosensory (gustatory) processes. Moreover astringency perception occurs on nongustatory mucosal surfaces and requires tissue movement to be perceived,<sup>21</sup> in agreement with a tactile mechanism involving an increase of in-mouth friction.

The present work explores the interactions of a common tannin, epigallocatechin gallate (EgCG), with a recombinant human salivary basic PRP, IB5. The sequence of IB5 and the structure of EgCG are shown in parts a and b of Figure 1. EgCG is a multidentate ligand able to bridge two proteins.<sup>27</sup> SAXS experiments have shown that IB5 takes unusually extended conformations compared to other IDPs.<sup>28</sup> Circular dichroism and NMR have given indications of disordered structures with short polyproline II helical sections that serve as anchorage for the binding of EgCG.<sup>29</sup> Studies of EgCG-IB5 interaction by dynamic light scattering, microcalorimetry, and circular dichroism led to **the proposal of a three-stage mechanism** involving binding of tannins to proteins, aggregation of the proteins when the tannin/protein molar ratio exceeds a threshold, and precipitation at still higher molar ratios.<sup>30</sup>

In the present work we address the following questions: (1) How strongly do EgCG molecules bind to IB5, how many binding sites are there on each protein, and what is the distribution of EgCG on these sites? (2) How many tannins are needed to cause aggregation of the proteins, what is the average

number of proteins per aggregate, and what is the structure of these aggregates?

The answers to these questions should provide a microscopic basis for understanding the physiological functions of proline-rich proteins, particularly the phenomena that take place in the mouth upon ingestion of tannin-rich foods or drinks.

Addressing these questions is challenging because IB5 has several binding sites leading to complex mixtures composed of IB5•EgCG complexes with several stoichiometries that may then react with each other. We used an approach combining mass spectrometry (MS), small-angle X-ray scattering (SAXS), and dynamic light scattering (DLS). At first we sorted out the single-protein complexes using MS. Indeed, MS distinguishes the different noncovalent complexes that coexist in solution.<sup>31,32</sup> Its performance in PRP–tannin interactions has been previously demonstrated.<sup>33–37</sup> Then we used SAXS to determine the conformations of the complexes, the structures of the aggregates, and their relative compositions. Finally we used DLS to determine the mass of protein per aggregate.

These phenomena depend on the concentrations of the various species. We note  $T$  the molar concentration of tannins (EgCG) in a solution, of which  $T_{\text{bound}}$  are bound to proteins and  $T_{\text{free}} = T - T_{\text{bound}}$  remain free in solution. We note  $P$  the total protein concentration, of which  $P_{\text{solution}}$  are nonaggregated proteins and  $P - P_{\text{solution}}$  are proteins forming multiprotein aggregates. The nonaggregated proteins comprise both free proteins and complexes made of one protein and different numbers (0, 1, 2, ...) of tannins. We note  $(T/P)$  the overall ratio of tannins to proteins in the solution, and  $(T_{\text{bound}}/P)$  the ratio of bound tannins to total proteins in the solution.

## ■ MATERIALS

The human salivary proline-rich protein IB5 was produced by the use of the yeast *Pichia pastoris* as a host organism and purified as previously described.<sup>28,38</sup> It was then freeze-dried and stored at  $-20$  °C until use. Epigallocatechin gallate (EgCG) was purchased from Sigma (Poole, UK) and ammonium acetate from Merck (Darmstadt, Germany). The ammonium acetate 50 mM buffer was prepared in Milli-Q-purified water, acidified to pH 5.5 with acetic acid, filtered at  $0.22$   $\mu\text{m}$ , and stored at  $4$  °C.

For SAXS and light scattering, filtered buffer was added to dry protein powder to yield a stock protein solution, and to EgCG powder to yield a stock tannin solution; both solutions were filtered again at  $0.45$   $\mu\text{m}$ , and then centrifuged until SAXS spectra indicated that no

protein aggregates remained in the stock IB5 solution. The protein solution in buffer was prepared at twice the final protein concentration, and the tannin solution at twice the final EgCG concentration. Then equal volumes of each were mixed and agitated on a vortex to reach final concentrations. The protein concentration was determined from the SAXS intensity at  $q \rightarrow 0$  (Supporting Information, section 3.1) and from the molar mass of the protein: it was 2.4 mg/mL or  $P = 0.336$  mM. For MS the concentrations of the protein solutions were 0.005 and 0.05 M and an ammonium acetate 1 mM buffer acidified to pH 5.5 was used.

The compositions of the solutions were varied over ranges that overlap the physiological ranges of concentrations. The total concentration of protein in saliva is in the range 1–3.5 mg/mL. Most of these proteins originate from the parotid gland. The PRPs are a large fraction (up to 70%) of this total. The concentration of IB5 used in SAXS experiments (2.4 mg/mL) was near the top of this range, and the concentrations used for MS were much below. For tannins, we know that the average concentration of EgCG in green tea is 0.27 mg/mL (0.1–1 range) or 0.590 mM (0.2–2 range). The SAXS and DLS experiments were performed in this range. The pH was slightly lower than that of stimulated saliva, which is comprised between 5.8 and 7.2,<sup>39</sup> as is the case when drinking wine or fruit juice. As the isoelectric point of IB5 is 11.2, the charge state of IB5 is expected to be the same in saliva and in our buffer. The ionic strength used is comprised in the saliva natural variations.<sup>40</sup>

## METHODS

At low protein concentration (0.005 and 0.050 mM) and low ionic strengths (1 mM) we observed the IB5•EgCG complexes using electrospray ionization mass spectrometry (ESI-MS) and confirmed their identity by tandem mass spectrometry (MS/MS) using a collision gas to activate precursor ions. At higher protein concentrations (0.21 to 0.42 mM) and high ionic strength (50 mM) we observed protein aggregation through dynamic light scattering (DLS) and small angle X-ray scattering (SAXS).

Mass spectrometry experiments were realized by using a linear ion-trap mass spectrometer (LTQ XL, Thermo Electron, San Jose, CA, USA) and a hybrid quadrupole time-of-flight (Q-TOF) Qstar Pulsar i mass spectrometer (ABSciex, Framingham, MA). Both instruments are equipped with an ESI ion source [56]. The solutions were infused directly into the mass spectrometer at a flow rate of 4  $\mu$ L/min in the positive ion mode. The mass spectrometer parameters were optimized to transfer the noncovalent complexes from the solution to the gas phase. The source voltage and tube lens voltage of the ion trap were set at 4.2 kV and 100 V, respectively, while the heated capillary temperature was set at 200 °C and the sheath gas flow rate at 20. The following parameters were used on the Q-TOF: the source voltage was set to 5.8 kV in positive ion mode, the declustering potential at 47 V, the focusing potential at 209 V, the declustering potential 2 at 17 V, the ion source gas 1 set at 22, the ion source gas 2 at 0, the curtain gas at 10, and the capillary was not heated up. Mass spectra were studied by using *mMass* software and Igor Pro (Wavemetrics, Portland, OR).

MS/MS experiments have been performed with use of both mass spectrometers. However, experiments with the ion-trap have been realized to confirm ion identification, while the Q-TOF has been used to establish the dissociation curves of the noncovalent complexes. For MS/MS experiments with the ion-trap, collision-induced dissociation (CID) was performed with helium as collision gas. Precursor ions were activated during 30 ms and at a percentage of normalized collision energy (% NCE) giving enough dissociation for ion identification. During MS/MS experiments in the Q-TOF, nitrogen was used as collision gas in the collision cell (Linac) with a CAD gas setting of 5. The collision-set energy voltage  $V_c$  was increased from 0 to 50 V. The kinetic energy of the precursor ion in the laboratory frame of reference is  $E_{lab} = zeV_c$ , where  $z$  is the number of charges on the ion and  $e$  is the charge of an electron.

SAXS experiments were performed with the SWING beamline at the synchrotron SOLEIL. The incident beam energy was 12.0 keV (wavelength 1.033 Å), the distance from the sample to the Avix CCD

detector was 1, 2, and 5 m, and the scattering vector  $q$  ranged from 0.002 to 1  $\text{\AA}^{-1}$ . Experiments were performed at 20 °C. Several successive frames (typically 10) of 0.5 s each were recorded for both sample and solvent. We checked that X-rays did not damage the proteins by comparing successive frames. The average intensity and experimental error of each set of frames were subsequently computed. Scattering from the solvent was measured and subtracted from the corresponding intensity of protein + tannin solution. DLS experiments were performed with a Malvern Nano ZS instrument, using 2  $\mu$ L scattering cells.

## RESULTS

**Visual Observations and Light Scattering.** *Visual Observations.* Immediately after mixing tannin (EgCG) solutions and protein (IB5) solutions, the samples were examined visually. For solutions made at high ionic strength (50 mM buffer), a slight turbidity was observed whenever the tannin concentration was above 1 mM, indicating that extensive aggregation took place. **Precipitation was observed at 2 mM EgCG.** Over times of the order of a day, the turbidity increased further, went through a maximum, and then decreased. On the other hand, there was no turbidity in samples made at low ionic strength (in 1 mM buffer). Also, we did not observe any aggregation in pure EgCG solutions at concentrations up to 2 mM and beyond. To obtain more precise and quantitative data on these aggregation processes, we used light scattering.

*Light Scattering from Protein + Tannin Solutions.* DLS experiments were performed to determine the number of proteins per aggregate. The solutions were made in the 50 mM buffer with  $P = 0.21$  and 0.42 mM protein and  $T = 0.05$  to 2.18 mM EgCG. Figure 2 presents the scattered intensities measured right after mixing, normalized by the intensity of a pure protein solution as follows. First the value of intensity/protein

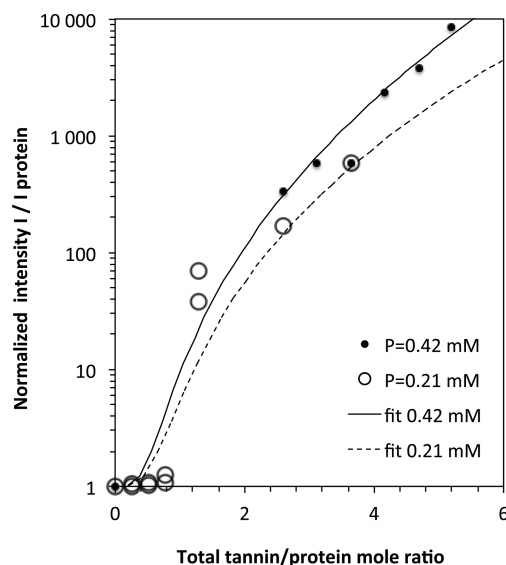


**Figure 2.** Light scattering by solutions of protein IB5 and tannin EgCG in the acetate buffer. The intensity values have been normalized by the intensity scattered by a pure protein solution of the same protein concentration  $P$ . The large values of the normalized intensities are from protein aggregates. The aggregation starts at a threshold in tannin concentration  $T = 0.2$  mM. Beyond this threshold, the normalized intensity grows nearly exponentially with  $T$ . The lines are theoretical predictions from a model in which dense aggregates have a core made of proteins that have bound at least 3 tannins each, and a surface made of proteins that have bound fewer tannins.

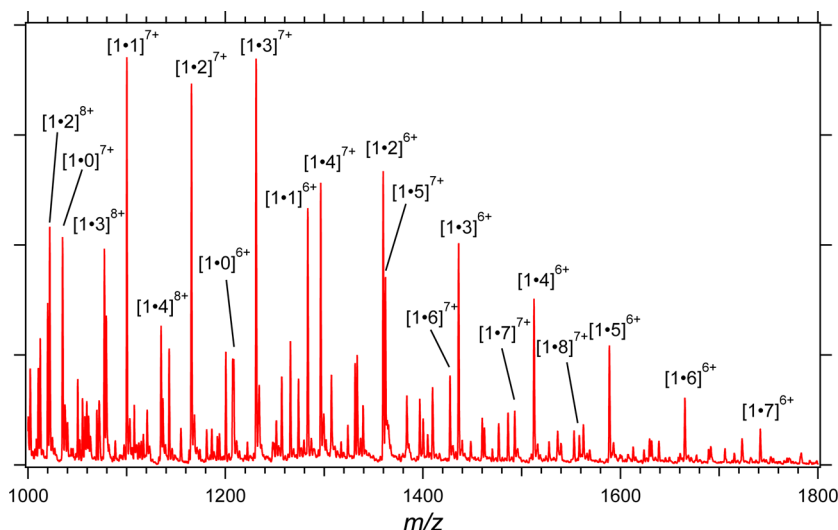


**Figure 3.** Positive ESI-MS spectrum of IB5 (0.05 mM)–EgCG (0.5 mM) mixture. The following caption is used  $[P\bullet K]^{C+}$  with respectively P and K the number of proteins and tannins involved in the molecular and supramolecular ions and C the charge state of ions.

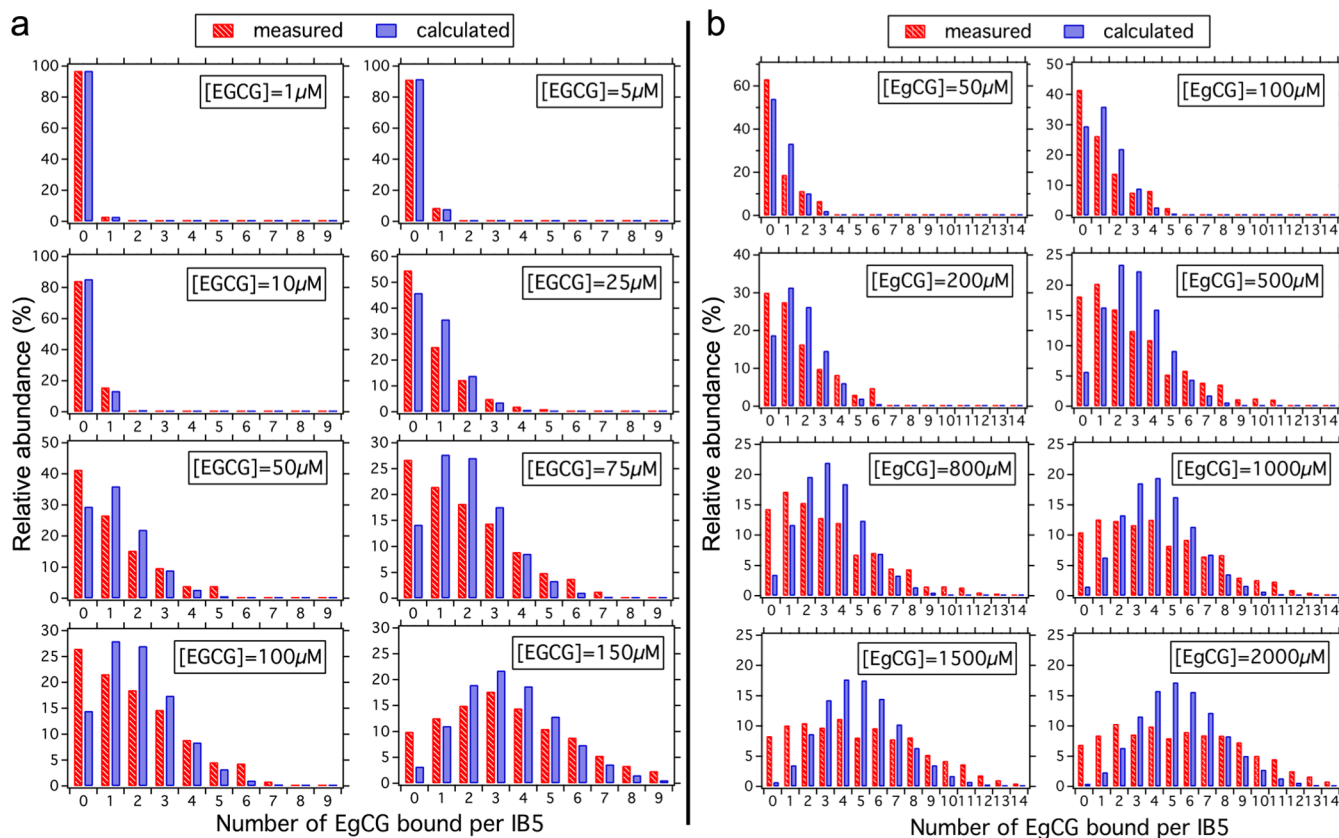


**Figure 4.** Distributions of bound EgCG on IB5 with (a) IB5 at 5  $\mu\text{M}$  and (b) IB5 at 50  $\mu\text{M}$ . Horizontal scale: number of bound tannins per protein. Vertical scale: frequencies of proteins that have respectively 0, 1, ..., 14 bound tannins. The red bars are the measured frequencies and the blue ones are the frequencies expected from the Poisson distribution. Each graph is for one concentration of EgCG.

concentration,  $I_{\text{prot}}/P$ , was determined for pure protein solutions and extrapolated to low protein concentrations. Then the values of  $I/P$  for the mixed protein + tannin solutions were measured and divided by that of the pure protein solution.

Three remarkable features emerged from these results. First, there was a threshold in tannin concentration  $T$ , below which the scattered intensities were practically identical with that of the pure protein solution. For solutions at  $P = 0.21$  mM, this

threshold was at  $T = 0.2$  mM (Supporting Information, section 1.1). Then, beyond this threshold, the scattered intensities were much higher ( $\times 100$  to  $\times 10\,000$ ) than those of the pure protein solutions, and they increased nearly exponentially with the tannin concentration  $T$ . At higher protein concentrations (0.42 mM) it took more EgCG to reach the same number of proteins per aggregate. Also, the hydrodynamic radii of these aggregates

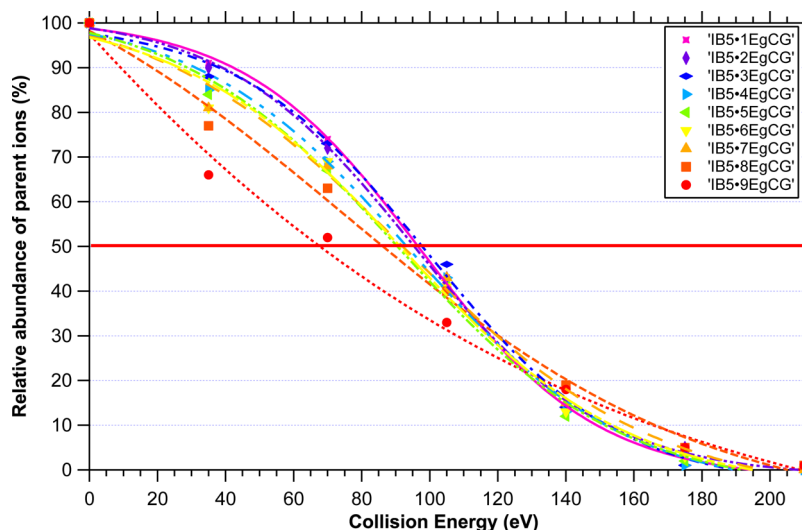


**Figure 5.** Dissociation curves of IB5•*k*EgCG complexes from *k* = 1 to 9.

were quite large, in the range 100–10000 Å (Supporting Information, section 1.3).

**Kinetic Effects.** At each composition, the intensity increased with time over a few hours, went through a maximum at about 4 times the initial intensity, and then decreased. The kinetics of restructuring was faster for lower EgCG concentrations (Supporting Information, section 1.2). At longer times, the intensity of light scattered by the aggregates decreased slowly but steadily, and the hydrodynamic diameters increased, indicating that the aggregates continued to dissociate and reorganize.

**Binding through Mass Spectrometry. Mass Spectrometry Experiments.** Mass spectrometry experiments were performed in order to follow the binding of EgCG on IB5. The experiments were performed by using a buffer with a weak ionic strength (1 mM) to conserve the IB5 cationic charges and therefore prevent the aggregation.

The mass spectrum obtained by electrospraying the protein solution displayed a series of protonated peaks corresponding to four IB5 isoforms (a, 6923.70 Da; b, 7238.60 Da; c, 7080.60 Da; d, 7481.80 Da) with charge states ranging from +5 to +10 (Supporting Information, section 2.1). We performed two series of experiments using solutions containing respectively 0.005 and 0.05 mM IB5 and tannin/protein ratios ranging from 1/5 to 40/1. Figure 3 shows the mass spectrum of the IB5–EgCG 0.05–0.5 mM mixture. Though crowded, the spectrum reveals free IB5 and IB5•*k*EgCG supramolecular complexes with several charge states. Complexes with stoichiometries ranging from *k* = 1 up to 8 tannins can be observed on this spectrum. However, mixtures having higher tannin concentration show complexes having *k* values up to 14. For high tannin concentration, the *k* value might not correspond to the number *n* of binding sites on IB5 as molecules of EgCG can stack on top of each other.

**Distributions of Tannins on Proteins.** For each mixture, the relative abundance (*R*) of the different species has been established via the measurement of their respective peak areas (*A*). Each peak area was normalized by the sum of the areas of all major species (eq 1).

$$R = \frac{A}{\sum_{i=1}^x A_i} \times 100 \quad (1)$$

As free IB5 and IB5•*k*EgCG complexes have different charge states, their relative abundance is the sum of the relative abundances of all charge states. The concentrations of bound and free EgCG were subsequently calculated knowing the IB5 concentration. Figure 4 shows the relative frequencies of proteins that have respectively 0, 1, ..., 14 bound EgCG molecules.

These populations can be compared with those expected for a purely statistical distribution of the EgCG molecules on independent and equivalent binding sites. Accordingly, if  $N_p$  proteins capture  $\lambda N_p$  EgCG molecules, where  $\lambda = T_{\text{bound}}/P$  is the average number of bound tannins per protein, the relative populations  $f(k)$  of proteins that have captured *k* EgCG are given by the Poisson distribution:

$$f(k) = \frac{\lambda^k \exp(-\lambda)}{k!} \quad (2)$$

We know the values of the binding ratio  $\lambda$  for each ESI/MS experiment, hence we can calculate the expected population distribution  $f(k)$  according to eq 2, and compare it with the measured distribution. This comparison is presented in Figure 4.

**Study of the IB5•EgCG Complexes through Tandem Mass Spectrometry Experiments.** As molecules of EgCG can stack on each other, the stoichiometries of IB5•*k*EgCG complexes cannot correspond to the number of binding sites. To determine the number of EgCG binding sites on IB5, we have performed CID MS/MS experiments using a Q-TOF. The IB5•*k*EgCG complexes from *k* = 1 to 9 have been selected and then activated by collision with a neutral gas (azote). For each complex, the collision energy was progressively increased until the full dissociation of the precursor ions. The relative intensity of the precursor ions was plotted against the collision energy giving the dissociation curves of each complex (Figure 5). The curves were fitted by using a Boltzmann sigmoidal function. From the curves, the collision energy at which half of the precursor ions are dissociated (*E*<sub>50</sub>) was determined to compare the stability of the complexes. IB5•*k*EgCG complexes from *k* = 1 to 8 present similar *E*<sub>50</sub>, while IB5•9EgCG complexes exhibit a smaller value. This observation indicates that above 8 tannins bound on IB5 a different type of

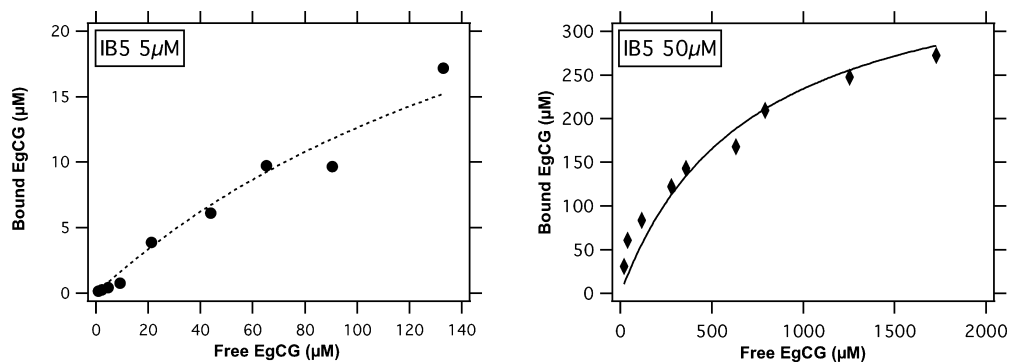


**Figure 6.** Binding isotherms of the tannins (EgCG) on the proteins (IB5, concentration  $P$ ). Horizontal scales: concentration of free tannins  $T_{\text{free}}$  in  $\mu\text{M}$ . Vertical scales: concentration of bound tannins  $T_{\text{bound}}$ . Left:  $P = 0.005$  mM. The data (dots) are fitted by the Langmuir model (dashed line) with  $n = 8$  binding sites per protein and a binding energy  $\Delta\mu_2 = 8.44RT_a$ . Right:  $P = 0.05$  mM. The data (diamonds) are fitted by the Langmuir model (solid line) with  $n = 8$  binding sites per protein and a binding energy  $\Delta\mu_2 = 7.26RT_a$ .

interaction, which is more labile, is involved. This second type of interaction could be the stacking of tannins.

**Binding Isotherms.** From the relative frequencies of proteins that have bound 1, 2, ..., 14 tannins, we have calculated the concentration  $T_{\text{bound}}$  of bound tannins, and then the concentration of free tannins  $T_{\text{free}} = T - T_{\text{bound}}$ .<sup>41,42</sup> These concentrations are presented in Figure 6.

The Langmuir model is the simplest way to describe the binding equilibrium of small molecules to a set of identical independent sites located on a macromolecule.<sup>43</sup> This model has two parameters, which are the concentration  $T_{\text{free}}$  of free tannins in the solution and the binding free energy per mole of bound tannins,  $\Delta\mu_{\text{free-bound}}$ , normalized by the energy of thermal agitation,  $RT_a$ . The equilibrium condition yields the fraction  $X_{\text{bound}}$  of sites on the proteins that are occupied by bound tannins:

$$X_{\text{bound}} = \frac{T_{\text{bound}}}{nP} = \frac{KT_{\text{free}}}{KT_{\text{free}} + 1}$$

with  $K = \exp\left(\frac{\Delta\mu_{\text{free-bound}}}{RT_a}\right)$  (3)

This is a relation between  $T_{\text{bound}}$  and  $T_{\text{free}}$ , with parameters  $n$ ,  $P$ , and  $K$ . We know the actual values of the concentrations  $T_{\text{bound}}$  and  $T_{\text{free}}$  from the MS experiments. Consequently we can search which values of  $n$  and  $K$  reproduce the actual relation between  $T_{\text{bound}}$  and  $T_{\text{free}}$ . The fit of the data shown in Figure 6 yields  $n = 8$  and  $\Delta\mu/RT_a = 8.44$  or  $K = 0.216$  mM for the solution with  $P = 0.005$  mM protein, and  $n = 8$  and  $\Delta\mu/RT_a = 7.26$  or  $K = 0.706$  mM for the solution with  $P = 0.05$  mM protein. The fact that the parameters  $n$  and  $\Delta\mu$  are so similar in both cases suggests that the Langmuir model is appropriate, i.e., the binding sites are independent and they have similar free energies.

**Small Angle X-ray Scattering. Aggregation of IB5 Caused by EgCG.** SAXS experiments were performed in order to study protein aggregation that occurred at higher ionic strength (50 mM acetate buffer), for the more concentrated protein solutions ( $P = 0.336$  mM), in the presence of tannins ( $T = 0.2$  to 4 mM). Two series of experiments were done at different times after the preparation of the solutions: 17 h at 10 °C for the first set of samples (presented below), and 6 h at 20 °C for the second set (Supporting Information, section 3.7), i.e., about the time of the maximum intensity according to light

scattering. In both cases SAXS experiments were performed at 20 °C. Both series gave very similar results.

Figure 7 presents the SAXS spectra for a series of solutions containing a fixed protein concentration ( $P = 0.336$  mM) and

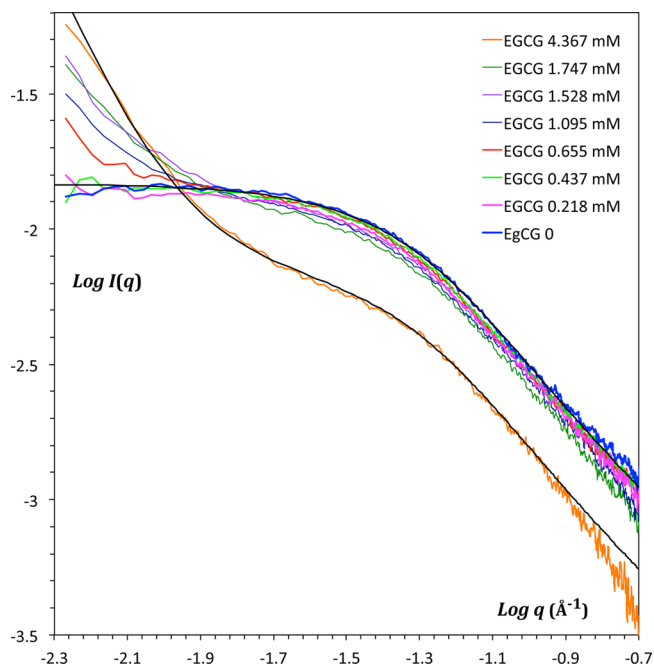


**Figure 7.** SAXS spectra from samples with the same protein concentration ( $P = 0.336$  mM) but different tannin concentrations (indicated in the figure). The scattering at  $q > 0.01$   $\text{\AA}^{-1}$  is mainly from nonaggregated proteins. The excess scattering at  $q < 0.01$   $\text{\AA}^{-1}$  signals the presence of dense protein aggregates. The spectrum of the solution containing proteins only (blue line) is fitted by the theoretical scattering curve for worm-like chains with parameters given in Table 1. A linear combination of nonaggregated proteins and large dense aggregates fits all other spectra. These samples were equilibrated for 17 h at 10 °C (see also the Supporting Information, section 3.7, for other equilibration times).

increasing concentrations of tannins ( $T = 0$  to 4.36 mM). The high- $q$  part of these spectra ( $q > 0.01$   $\text{\AA}^{-1}$ ) is slowly varied with  $q$  (slower than  $q^{-2}$ ); we argue below that it is characteristic of nonaggregated proteins with highly extended conformations.<sup>28</sup> The low- $q$  part ( $q < 0.01$   $\text{\AA}^{-1}$ , dimensions  $r > 600$   $\text{\AA}$ ) has a fast variation with  $q$  (close to  $q^{-3}$ ), which signals the presence of

very large objects, i.e., aggregates. In this  $q$  range the intensities rise rapidly with EgCG concentration when it exceeds  $T = 0.5$  mM.

**Conformations of Proteins with Bound Tannins.** We found that each spectrum could be fitted by a linear combination of the scattering from aggregates (first term) and that from nonaggregated proteins in solution (second term):

$$I(q) = CK(q) + DH(q) \quad (4)$$

The following analysis aims to reproduce the complete set of spectra with the smallest number of parameters, while keeping these parameters meaningful. Regarding the first term, we found that all  $K(q)$  functions can be approximated by power laws with the same exponent  $-d_f = -3$ . Since we do not know precisely the aggregates sizes,  $K(q)$  is an empirical function chosen to match the scattering, and  $C$  is proportional to the concentration of aggregates.

Regarding the second term, it must contain contributions from proteins that have bound either 0, 1, 2, ... or  $k$  tannins:

$$H(q) = f_0 H_0(q) + f_1 H_1(q) + \dots + f_k H_k(q) \quad (5)$$

The frequencies  $f_k$  can be deduced from the MS results, and the form factors  $H_k(q)$  could be calculated for thick worm-like chains similar to the pure protein in solution, but taking into account the contribution of the bound tannins. However, the number of parameters of this model would be excessively large. Indeed, it takes 3 parameters to describe each form factor, so that if the solution contained proteins with, say, 0, 1, 2, 3, and 4 bound tannins, it would take 15 parameters to determine the second term of eq 5. The precision of the data does not warrant this. We notice that the spectra obtained at different compositions are nearly identical at high  $q$  values (Figure 7). Therefore, at each composition, we can use a single form factor  $H(q)$ , calculated for a thick worm-like chain with a persistence length, as we did previously for the pure protein solutions,<sup>28</sup> and a single coefficient  $D$  (discussed in the next section):

$$\frac{H^{SB}(q)}{H^{SB}(q \rightarrow 0)} = g(x) + \frac{b}{L} \left[ \frac{4}{15} + \frac{7}{15x} - \left( \frac{11}{15} + \frac{7}{15x} \right) \exp(-x) \right] \quad (6)$$

$$g(x) = 2(e^{-x} + x - 1)/x^2 \quad (7)$$

where  $x$  is equal to  $(q^2 L b)/6$ ,  $b$  is the length of the statistical element, and  $L$  is the contour length of the chain.<sup>28</sup> Finally we take into account the thickness of the worm-like chain through a factor that depends on the radius  $R_c$  of its cross section:

$$H(q) = H^{SB}(q) \exp\left(\frac{-q^2 R_c^2}{2}\right) \quad (8)$$

Figure 8 shows the fits to two spectra according to eqs 4–8, with the parameters  $C$ ,  $D$ ,  $L$ ,  $b$ , and  $R_c$  adjusted for each spectrum (as in Figure 7). The spectra are from a solution at low EgCG concentration ( $T = 0.437$  mM) and a solution at high EgCG concentration ( $T = 1.747$  mM). They are plotted in the Kratky representation,  $q^2 I(q)$  vs  $q$ , which enhances the effects of structural differences between chains with different numbers of bound tannins. The other spectra have been fitted in the same way. Table 1 lists the values of the structural parameters extracted from all such fits. Only one of these

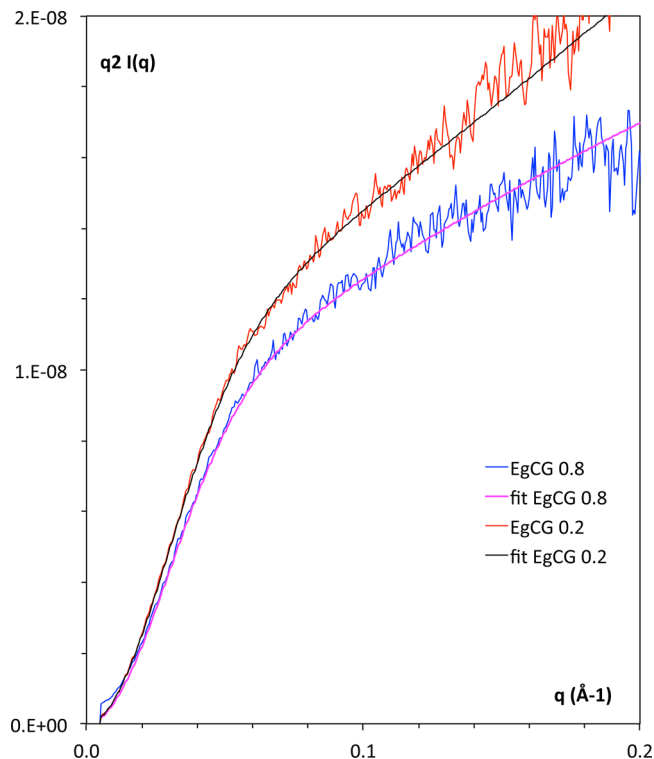


**Figure 8.** SAXS spectra of IB5–EgCG solutions, plotted in the Kratky representation,  $q^2 I(q)$  vs  $q$ . This representation enhances the high  $q$  part of the spectra, where the scattering originates from nonaggregated proteins that have remained in the solution. Upper set of data: solution containing  $T = 0.437$  mM of the tannin EgCG and  $P = 0.336$  mM of the salivary protein IB5. Lower set of data:  $T = 1.747$  mM and  $P = 0.336$  mM.

**Table 1. Geometrical Parameters Used to Fit the SAXS Spectra with a “Thick Worm-Like Chain” Model<sup>a</sup>**

$T_i$ mg/mL	$T$ , mM	$T_{\text{bound}}/P$	$L$	$b$	$R_g$	$R_c$
0	0	0	$207 \pm 10$	$30 \pm 1$	29.2	$2.7 \pm 0.4$
0	0	0	$207 \pm 10$	$32 \pm 1$	29.9	$2.4 \pm 0.4$
0.1	0.218	0.507	$207 \pm 15$	$31 \pm 2$	29.6	$2.7 \pm 0.4$
0.2	0.437	1	$207 \pm 15$	$31 \pm 2$	29.6	$2.8 \pm 0.4$
0.3	0.655	1.473	$207 \pm 15$	$30 \pm 2$	29.2	$2.9 \pm 0.4$
0.5	1.095	2.371	$207 \pm 15$	$29 \pm 2$	28.9	$3.3 \pm 0.4$
0.7	1.528	3.168	$190 \pm 15$	$33 \pm 2$	28.8	$3.2 \pm 0.4$
0.8	1.747	3.533	$200 \pm 15$	$32 \pm 2$	29.5	$3.7 \pm 0.4$
2	4.367	6.124	$200 \pm 15$	$30 \pm 2$	28.8	$3.8 \pm 0.4$

<sup>a</sup>The parameters are in Å:  $L$ , contour length of the chain,  $b$ , length of the statistical segment,  $R_g$ , overall radius of gyration, and  $R_c$  radius of the cross-section of the chain. The compositions are specified by  $T$ , total tannin concentration, and  $P = 0.336$  mM;  $T_{\text{bound}}/P$  is the molar ratio of bound tannins to total proteins, calculated from the adsorption isotherm determined through MS. For the pure protein solutions there are slight differences with respect to the value of  $L$  given previously,<sup>28</sup> due to differences in the populations of the four IB5 isoforms. The two rows at  $T = 0$  correspond to different experiments, and the differences between them give an idea of their precision.

parameters has systematic variations: as the number of bound tannins per protein increases, the chains become thicker (larger cross-section). This makes sense, since the tannins have a high contrast and are bound as side groups of the main polypeptide chain.

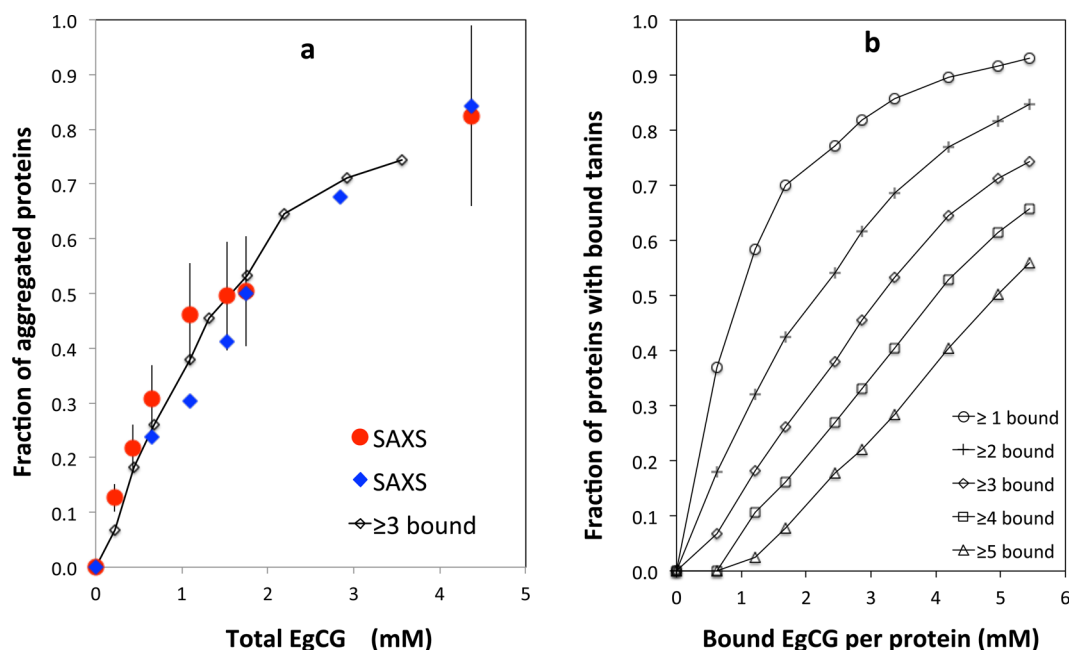


**Figure 9.** (a) Fraction of proteins that are aggregated, calculated from SAXS (filled dots and filled diamonds are from two experiments), and comparison with MS results from solutions that do not aggregate (open diamonds, proteins that have bound at least 3 EgCG molecules). Horizontal scale: total tannin (EgCG) concentration in mM. It is argued that it takes at least 3 tannins per protein to collapse the proteins into dense aggregates. (b) Fraction of proteins that have bound a set number of tannin molecules, from mass spectrometry. The horizontal axis is the average number of bound tannins per protein,  $T_{\text{bound}}/P$ , calculated from the Langmuir fit to the MS data.

**Protein Aggregation.** We calculate the fraction of nonaggregated proteins from the relative magnitude of the scattered intensities. For this purpose we extract from the worm-like chain fit (eqs 6–8) the intensity scattered by the proteins in the solution containing  $T$  tannins, and compare it with that from the pure protein solution. If proteins that have 0, 1, ...,  $k$  bound tannins coexist in the solution, the intensity scattered at  $q \rightarrow 0$  by these proteins is:

$$H(T, q \rightarrow 0) = H(T = 0, q \rightarrow 0) \frac{P_{\text{solution}}}{P} \frac{\sum_{i=0}^k \alpha_i f_i}{\sum_{i=0}^k f_i} \quad (9)$$

where  $P_{\text{solution}}$  is the concentration of nonaggregated proteins in the solution,  $H_i(q \rightarrow 0)$  is the intensity extrapolated to  $q \rightarrow 0$  from proteins that have bound  $i$  tannins,  $f_i$  is the fraction of such proteins, from MS, and  $\alpha_i$  is the ratio of scattered intensity between a protein that has bound  $i$  tannins and a protein that has none (Supporting Information, sections 3.1 to 3.4):

$$\alpha_i = \frac{H_i(q \rightarrow 0)}{H_0(q \rightarrow 0)} = \left[ 1 + i \frac{\nu_t \Delta \rho_t}{\nu_p \Delta \rho_p} \right]^2 \quad (10)$$

where  $\nu_t$  is the volume of a tannin and  $\nu_p$  is that of a protein, and  $\Delta \rho_t$  is the scattering density of a tannin and  $\Delta \rho_p$  is that of a protein. Thus we extract  $P_{\text{solution}}/P$  from eqs 9 and 10 and obtain the fraction of aggregated proteins as  $1 - P_{\text{solution}}/P$  (Supporting Information, sections 3.5 to 3.9). The variation of this fraction is presented in Figure 9a and Table 2, as a function of the total tannin concentration. At this point we note that adding 0.2 mM EgCG is enough to aggregate a significant fraction of the proteins, in agreement with the light-scattering result (Figure 2).

**Kinetics of Aggregation and Dissociation.** Similar sets of SAXS spectra were obtained at different times after mixing

**Table 2. Concentrations of Aggregated and Nonaggregated Proteins According to SAXS Data<sup>a</sup>**

$T$ , mM	$T_{\text{free}}$ , mM	$T_{\text{bound}}$ , mM	$T_{\text{bound}}/P$	$P_{\text{aggregated}}$ , mM	$P_{\text{solution}}$ , mM
0	0	0	0	0.000	0.336
0.218	0.048	0.170	0.51	0.043	0.293
0.437	0.101	0.336	1.00	0.073	0.263
0.655	0.160	0.495	1.47	0.103	0.233
1.095	0.298	0.797	2.37	0.155	0.181
1.528	0.463	1.065	3.17	0.166	0.170
1.747	0.559	1.188	3.53	0.169	0.167
4.367	2.309	2.058	6.13	0.277	0.059

<sup>a</sup> $T$  is the total tannin concentration (EgCG).  $T_{\text{free}}$  and  $T_{\text{bound}}$  are the concentrations of free and bound tannins, calculated according to the MS results.  $T_{\text{bound}}/P$  is the number of bound tannins per protein with  $P = 0.336$  mM the total protein concentration.  $P_{\text{aggregated}}$  is the concentration of aggregated proteins and  $P_{\text{solution}}$  the concentration of nonaggregated proteins, both calculated by fitting the experimental spectra according to eqs 4–10.

the protein solutions with the tannin solution (Figure 8, Supporting Information). In all cases, a linear combination of nonaggregated proteins and dense aggregates fits all spectra, according to eqs 4–10. The amounts of aggregated proteins were highest at short times after mixing. At very long times, on the order of a day, all these aggregates were found to dissociate spontaneously to some extent, as also observed through DLS (Supporting Information, section 1.2).

## DISCUSSION

**Aggregating and Nonaggregating Solutions.** The aim of this discussion is to relate binding data, obtained from MS, and structural data, obtained from SAXS and DLS. Scattering experiments have been performed in 50 mM acetate buffer, which has an ionic strength similar to that occurring in the

mouth. In these conditions, the cationic charges of the proteins are screened, and the proteins may aggregate through bridges created by bound EgCG molecules. The MS data were obtained under 1 mM salt added to the protein + tannin mixture, owing to the poor tolerance of electrospray ionization to salts. However, mass spectrometry has been used only to study the interaction of the ligands to proteins, which is not affected by ionic strength. The results from both sets of experiments may then be related with confidence.

**The Population of Protein Aggregates.** When two species combine to form aggregates, the first question is: How many different types of aggregates are there, in terms of compositions and structures? This question is quite difficult to answer, since there must be variations in the numbers of tannins (EgCG) and proteins (IB5) per aggregate, and in the resulting structures. Hence a detailed description of the ensemble of aggregates is out of reach. However, we can answer a simpler question, which is whether the collection of aggregates can be meaningfully described as a single population, or else as two coexisting populations.

The SAXS data presented in Figure 7 and the fits according to eq 4 show that the solutions contain two populations, i.e., “dense” aggregates coexisting with nonaggregated proteins. Let us first discuss the population of nonaggregated proteins. The SAXS results show that these proteins have similar conformations to the proteins in pure IB5 solutions. However, the increasing values of the cross section of the polypeptide chains (Table 1) indicate that these proteins have bound a significant number of tannin molecules. The scattered intensities have been analyzed according to a simplified model where these proteins have bound the numbers of tannins that are predicted by the adsorption isotherm. This is adequate when most proteins are still nonaggregated. We find that the population of nonaggregated proteins decays continuously with rising tannin concentrations (Table 2 and Figure 9a). This decay matches the growth of the population of proteins that have bound at least 3 tannins (determined from MS), suggesting that they vanish from the solution.

Next, we consider the population of aggregates. First we focus on the composition  $P = 0.336$  mM,  $T = 0.5$  mM, for which the scattering from aggregates shows up in the low- $q$  part of the spectra (Figure 7). According to the analysis of SAXS data (Table 2), 20% of the proteins were aggregated and no longer contributed to the high- $q$  solution scattering. We know from MS how the tannins were initially distributed on the proteins before aggregation took place: for the corresponding composition with the same concentration of free EgCG, the frequencies of proteins that have respectively 1, 2, 3, 4, 5 bound EgCG molecules are 26%, 14%, 8%, 8%, and 3% (Table V, Supporting Information). The SAXS result is recovered if it is assumed that all proteins with at least 3 bound tannins did aggregate. The same correspondence is obtained at other compositions, indicating that the proteins with at least 3 bound tannins form the aggregates.

This result is in quantitative agreement with those of Pascal et al.<sup>29</sup> and Poncet-Legrand et al. obtained with polyproline as a protein<sup>30,44</sup> and those of Charlton et al. with proline-rich peptides.<sup>45</sup> As EgCG is a multidentate ligand, it may form bridges between proteins within aggregates, leading to the collapse of highly connected aggregates. This is in agreement with the fractal exponent of the aggregate structure, measured by SAXS, which is  $d_f = 3$ , characteristic of dense particles. At first, this dense structure may seem to conflict with the large

hydrodynamic radii measured through DLS, which grow as the square root of the mass per aggregate (rather than the cube root law expected for dense particles). This conflict is resolved by considering that the aggregates have a dense core (seen by SAXS) and a less dense corona, which controls their hydrodynamic properties measured by DLS.

**A Simple Poisoned Growth Model for Calculating the Aggregate Size.** Here we present a simple model of the protein + tannin aggregates, in order to calculate the number of proteins per aggregate, and predict the intensity of scattered light. This model is based on the idea that aggregates recombine (and therefore grow to larger sizes) until their surfaces are “poisoned” by unreactive species.<sup>46</sup> To keep the numbers of parameters to a minimum, we assume that all aggregates are identical, with the same radius and the same number of proteins. We further assume that each aggregate is made of a dense core that contains a high concentration of bridging tannins, and a corona made of proteins with few bridging tannins. Two aggregates may recombine during their collisions, if their surfaces carry enough tannin molecules to bridge them together. However, there is a large pool of proteins that carry few tannin molecules. As the aggregates grow, their surfaces capture a small fraction of these proteins, and they become unable to make permanent bonds to each other. Consequently the final sizes of aggregates are limited by the abundance of “poisons”, i.e., proteins that do not carry enough tannin molecules to continue the growth process.

Consider a solution containing  $N$  proteins, with a distribution  $f(k)$  of tannin molecules on these proteins. The proteins with  $k > k_0$  are aggregated, and they have formed a set of  $N_{ag}$  aggregates. Let  $n_{core}$  be the number of proteins in the core of each aggregate,  $V_{core}$  the volume of this core, and  $V^*$  the volume per protein in this core. Some of the proteins with  $k < k_0$  are at the aggregate surface (fraction  $\alpha$ ), but most of them are free in the bulk solution (fraction  $1 - \alpha$ ). Let  $n_{surface}$  be the number of proteins at the surface of the aggregate,  $A_{core}$  the area of the core surface, and  $A^*$  the surface area per protein in this surface layer. Let  $n_{solution}$  be the number of free proteins per aggregate. The distribution of proteins must verify the following sum rules:

$$n_{core} = \frac{V_{core}}{V^*} = \frac{N}{N_{ag}} \left[ 1 - \sum_{k=0}^{k=k_0} f(k) \right] \quad (11)$$

$$n_{surface} = \frac{A_{core}}{A^*} = \alpha \frac{N}{N_{ag}} \left[ \sum_{k=0}^{k=k_0} f(k) \right] \quad (12)$$

$$n_{solution} = (1 - \alpha) \frac{N}{N_{ag}} \left[ \sum_{k=0}^{k=k_0} f(k) \right] \quad (13)$$

$$n_{core} + n_{surface} + n_{solution} = \frac{N}{N_{ag}} \quad (14)$$

For a globular aggregate, the volume and surface area are related by  $V_{core}^2 A_{core}^{-3} = 1/36\pi$ , which may be rewritten as:

$$V_{core} = 36\pi \left( \frac{V_{core}}{A_{core}} \right)^3 \quad (15)$$

Hence it is easy to calculate  $n_{core}$  and  $n_{surface}$

$$n_{\text{core}} = 36\pi \frac{(V^*)^2}{(\alpha A^*)^3} [\phi(k)]^3$$

$$\text{with } \phi(k) = \left[ 1 - \frac{\sum_{k=0}^{k=k_0} f(k)}{\sum_{k=0}^{k=k_0} f(k)} \right] \quad (16)$$

$$n_{\text{surface}} = 36\pi \frac{(V^*)^2}{\alpha^2 (A^*)^3} [\phi(k)]^2 \quad (17)$$

Beyond this point, it is necessary to obtain some information on the parameter  $\alpha$ , which contains the information on the poisoning process. Fortunately this problem has already been studied in another context, for the poisoned growth of oil droplets in surfactant solutions.<sup>46</sup> The conclusions from that work are that  $\alpha$  and  $n_{\text{core}}$  are power laws of the poisoning ratio  $\phi(k)$ , so that:

$$n_{\text{core}} = n_0 [\phi(k)]^\beta \quad (18)$$

The exponent obtained for  $n_{\text{core}}$  through numerical simulation is  $\beta = 2.5$ .<sup>46</sup> To apply these predictions to the growth of protein aggregates bridged by tannin molecules, we assume that the distribution  $f(k)$  is the Poisson distribution given in eq 2. With this distribution, the data are best fitted by  $n_{\text{core}} + n_{\text{surface}}$  with  $\alpha \ll 1$ ,  $k_0 = 3 \pm 1$ , and  $\beta = 2 \pm 0.5$  (Figure 2). This power law reproduces the aggregation threshold and also provides a good fit to the rest of the data for both protein concentrations. The aggregation threshold is rather insensitive to the choice of parameters, and determined mainly by the tannin concentration at which there is a substantial frequency of proteins with at least 3 bound tannins (Figure 9b). Moreover the model reproduces well the fact that, beyond the aggregation threshold, the aggregates readily reach very large aggregation numbers. Accordingly the poisoned growth model does reproduce the aggregation of proteins by tannins.

**Aggregation Followed by Dissociation.** Over very long times, the mixed solutions show a slow rise in turbidity followed by an even slower decay of turbidity. The rise in turbidity may be caused by the continued recombination of aggregates, due to their Brownian collisions. Indeed the rate of increase of the intensity of scattered light matches that expected for a cluster–cluster aggregation process with a low efficiency of encounters (1 successful recombination in  $3 \times 10^6$ ). This is not surprising, given that the proteins and tannins must be in particular configurations in order to create a bridge.

The slow dissociation observed at long times, followed by spontaneous redispersion, may be caused by a redistribution of the tannins among the available proteins. Indeed, molecular dynamics simulations of the binding of EgCG to IB5 suggest that the tannin molecules may move fairly easily along the polypeptide chain.<sup>47</sup> For a tannin concentration that is twice the aggregation threshold, the total number of bound tannins amounts to  $T_{\text{bound}}/P = 1$  tannin per protein. If the tannins do redistribute uniformly among all proteins, there will no longer be any proteins with 3 or more bound tannins, and therefore the aggregates will dissociate, expand, and dissolve, as observed. In addition, some tannins may change their connectivity from a configuration where they bridge two distinct proteins to a configuration where they bridge two sites of the same protein. This will reduce the number of bridges holding the aggregate together and lead to dissociation and dissolution of the aggregates.

## CONCLUSION

In this work we examined the binding of molecules of the tannin EgCG to a basic proline-rich salivary protein, IB5, the subsequent aggregation of the protein through bridging tannins, and the growth of the aggregates, determined by the distribution of tannins on the proteins (poisoned growth). We obtained a quantitative description of these processes, at the microscopic scale. These processes appear to be general. Thus this description could serve as a model for the interactions of other disordered proteins (e.g., other salivary proteins) with tannins or with other bridging ligands.

(1) In very dilute IB5–EgCG solutions of low ionic strength (1 mM) the proteins repel each other. In these conditions the tannins bind to individual proteins but do not cause any aggregation. Using mass spectrometry, we have determined the distribution of bound EgCG among all the proteins in solution, i.e., how many proteins have 1, or 2, or 3, ... bound EgCG molecules. This distribution is close to the Poisson (= random) distribution, thereby indicating that the sites on the protein are equivalent and independent. The number of binding sites is  $n = 8$ , which matches the number of short proline repeats on the polypeptide chain. The number of bound EgCG molecules follows a Langmuir adsorption isotherm with an equilibrium constant  $K_d = 0.706$  mM, or a free energy of  $7.26 \pm 0.5 RT_a$ , where  $RT_a$  is the energy of thermal agitation at 20 °C. This free energy is in between those found previously for proline-rich peptides by Charlton et al.<sup>45</sup> and for poly(L-proline) by Poncet-Legrand et al.<sup>44</sup> The differences are presumably due to the lengths of the polyproline sequences in each case.

(2) In solutions that are more concentrated and at higher ionic strength (acetate buffer 50 mM, pH 5.5), the binding of the tannins causes the protein to aggregate. DLS experiments indicate that the aggregation threshold is at a tannin concentration of 0.2 mM (with 0.21 mM protein). Comparing SAXS and MS results, we found that the proteins that have bound at least 3 EgCG molecules connect to each other through EgCG bridges and build the aggregates, in good agreement with the results of Poncet-Legrand et al.<sup>30,44</sup> and Charlton et al.<sup>45</sup> These aggregates recombine into larger ones until their growth is limited by adsorption of proteins that have bound fewer EgCG molecules, as described by the poisoned growth model. Through this process, the aggregates become quite large at concentrations that are not much higher than the threshold (up to 1000 proteins per aggregate at a total EgCG concentration of 1 mM). These results are consistent with the observation of hazes in protein–polyphenol systems.<sup>48</sup>

(3) The threshold for the formation of these aggregates is in a range of compositions that matches the physiological ranges: it is at 0.2 mM EgCG for 0.21 mM protein, and 0.5 mM EgCG for 0.42 mM IB5. This suggests that the aggregation of salivary proteins by tannins in the mouth could have a physiological function. An obvious function could be the regulation of the amount of free tannins in the ingested food and drinks.

(4) Another function for the aggregation of salivary proteins by tannins in the mouth could be to cause astringency. From the present results, we can find out if the ranges of concentration for the perception of astringency correlate with those where aggregation and precipitation take place. Astringency perception has been reported at EgCG concentrations in the range 0.2 mM<sup>49</sup> to 0.4 mM.<sup>50</sup> These values are remarkably close to the aggregation threshold that we found (0.2 mM EgCG in an IB5 solution of concentration 0.21 mM).

Moreover, we have demonstrated that this aggregation process readily leads to massive aggregates when tannins concentrations exceed the threshold. These cationic aggregates could then bind to the salivary film that covers the mucosa,<sup>51</sup> and trigger the astringency perception. Experiments on acid-treated saliva have evidenced a pathway that involves the preferential binding of tannins to acidic PRPs and statherins, which are also involved in the salivary film,<sup>52</sup> causing their aggregation.<sup>53</sup> This aggregation may then lead to a cascade of other phenomena at the colloidal scale, with involvement of the cationic bPRP at a later stage, and then precipitation or deposition of the cationic aggregates on the anionic mucosa. Experiments similar to those reported here but involving mixtures of 2 or more proteins could make it possible to find out which ones of these pathways are active in the mouth.

## ■ ASSOCIATED CONTENT

### ● Supporting Information

Additional results including time evolution of the scattered intensities in light scattering and SAXS, mass spectra of IB5 solutions, tables of frequencies of all protein populations as determined through MS, and expressions for the scattering by proteins in solution with bound tannins. This material is available free of charge via the Internet at <http://pubs.acs.org>.

## ■ AUTHOR INFORMATION

### Corresponding Author

\*Email: [bcabane@pmmh.espci.fr](mailto:bcabane@pmmh.espci.fr).

### Notes

The authors declare no competing financial interest.

## ■ ACKNOWLEDGMENTS

We thank Thérèse Marlin for production and purification of protein IB5. This work was supported by grant 07-BLAN-02 "PROTANIN" from Agence Nationale de la Recherche.

## ■ REFERENCES

- (1) Wright, P. E.; Dyson, H. J. Intrinsically Unstructured Proteins: Re-assessing the Protein Structure–Function Paradigm. *J. Mol. Biol.* **1999**, *293*, 321–331.
- (2) Dunker, A. K.; Brown, C. J.; Lawson, J. D.; Iakoucheva, L. M.; Obradovic, Z. Intrinsic Disorder and Protein Function. *Biochemistry* **2002**, *41*, 6573–6582.
- (3) Ward, J. J.; Sodhi, J. S.; McGuffin, L. J.; Buxton, B. F.; Jones, D. T. Prediction and Functional Analysis of Native Disorder in Proteins from the Three Kingdoms of Life. *J. Mol. Biol.* **2004**, *337*, 635–645.
- (4) Uversky, V. N.; Dunker, A. K. Understanding Protein Non-Folding. *Biochim. Biophys. Acta* **2010**, *1804*, 1231–1264.
- (5) Brown, C. J.; Johnson, A. K.; Dunker, A. K.; Daughdrill, G. W. Evolution and Disorder. *Curr. Opin. Struct. Biol.* **2011**, *21*, 441–446.
- (6) Williamson, M. P. The Structure and Function of Proline-Rich Regions in Proteins. *Biochem. J.* **1994**, *297*, 249–260.
- (7) Tompa, P. Intrinsically Unstructured Proteins Evolve by Repeat Expansion. *BioEssays* **2003**, *25*, 847–855.
- (8) Carlson, D. M. Salivary Proline-Rich Proteins: Biochemistry, Molecular Biology, and Regulation of Expression. *Crit. Rev. Oral Biol. Med.* **1993**, *4*, 495–502.
- (9) Bennick, A. Interaction of Plant Polyphenols with Salivary Proteins. *Crit. Rev. Oral Biol. Med.* **2002**, *13*, 184–196.
- (10) Lu, Y.; Bennick, A. Interaction of Tannin with Human Salivary Proline-Rich Proteins. *Arch. Oral Biol.* **1998**, *43*, 717–728.
- (11) Mehansho, H.; Butler, L. G.; Carlson, D. M. Dietary Tannins and Salivary Proline-Rich Proteins. Interactions, Induction and Defense Mechanisms. *Annu. Rev. Nutr.* **1987**, *7*, 423–440.
- (12) Mehansho, H.; Ann, D. K.; Butler, L. G.; Rogler, J. C.; Carlson, D. M. Induction of Proline-Rich Proteins in Hamster Salivary Glands by Isoproterenol Treatment and Unusual Growth Inhibition by Tannins. *J. Biol. Chem.* **1987**, *262*, 12344–12350.
- (13) Haslam, E. Polyphenol–Protein Interactions. *Biochem. J.* **1974**, *139*, 285–288.
- (14) Haslam, E.; Lilley, T. H.; Cai, Y.; Martin, R.; Magnolato, D. Traditional Herbal Medicines – The Role of Polyphenols. *Planta Med.* **1989**, *55*, 1–8.
- (15) Breslin, P. A. S.; Gilmore, M. M.; Beauchamp, G. K.; Green, B. G. Psychophysical Evidence that Oral Astringency is a Tactile Sensation. *Chem. Senses* **1993**, *18*, 405–417.
- (16) Baxter, N. J.; Lilley, T. H.; Haslam, E.; Williamson, M. P. Multiple Interactions between Polyphenols and a Salivary Proline-Rich Protein Repeat Result in Complexation and Precipitation. *Biochemistry* **1997**, *36*, 5566–5577.
- (17) Bate-Smith, E. C. Astringency in Foods. *Food* **1954**, *23*, 124.
- (18) Freitas, V. D.; Mateus, N. Protein/Polyphenol Interactions: Past and Present Contributions. Mechanisms of Astringency Perception. *Curr. Org. Chem.* **2012**, *16*, 724–746.
- (19) Bajec, M. R.; Pickering, G. J. Astringency: Mechanisms and perception. *Crit. Rev. Food Sci. Nutr.* **2008**, *48*, 858–875.
- (20) Lee, C. B.; Lawless, H. T. Time Course of Astringent Sensations. *Chem. Senses* **1991**, *16*, 225–238.
- (21) Rossetti, D.; Yakubov, G. E.; Stokes, J. R.; Williamson, A.-M.; Fuller, G. G. Interaction of Human whole Saliva and Astringent Dietary Compounds Investigated by Interfacial Shear Rheology. *Food Hydrocolloids* **2008**, *22*, 1068–1078.
- (22) Rossetti, D.; Bongaerts, J. H. H.; Wantling, E.; Stokes, J. R.; Williamson, A.-M. Astringency of Tea Catechins: More than an Oral Lubrication Tactile Percept. *Food Hydrocolloids* **2009**, *23*, 1984–1992.
- (23) Obreque-Slier, E.; Lopez-Solis, R.; Pena-Neira, A.; Zamora-Marín, F. Tannin-Protein Interaction is more closely Associated with Astringency than Tannin-Protein Precipitation: Experience with two Oenological Tannins and a Gelatin. *Int. J. Food Sci. Technol.* **2010**, *45*, 2629–2636.
- (24) Schiffman, S. S.; Suggs, M. S.; Sostman, A. L.; Simon, S. A. Chorda Tympani and Lingual Nerve Responses to Astringent Compounds in Rodents. *Physiol. Behav.* **1992**, *51*, 55–63.
- (25) Critchley, H. D.; Rolls, E. T. Responses of Primate Taste Cortex Neurons to the Astringent Tannic Acid. *Chem. Senses* **1996**, *21*, 135–145.
- (26) Iiyama, S.; Ezaki, S.; Toko, K.; Matsuno, T.; Yamafuji, K. Study of Astringency and Pungency with Multichannel Taste Sensor Made of Lipid Membranes. *Sens. Actuators, B* **1995**, *24*, 75–79.
- (27) Jöbstl, E.; O'Connell, J.; Fairclough, P. A.; Williamson, M. P. Molecular Model for Astringency Produced by Polyphenol/Protein Interactions. *Biomacromolecules* **2004**, *5*, 942–949.
- (28) Boze, H.; Marlin, T.; Durand, D.; Perez, J.; Vernhet, A.; Canon, F.; Sarni-Manchado, P.; Cheynier, V.; Cabane, B. Proline-Rich Salivary Proteins have Extended Conformations. *Biophys. J.* **2010**, *99*, 656–665.
- (29) Pascal, C.; Pate, F.; Cheynier, V.; Delsuc, M. A. Study of the Interactions Between a Proline-Rich Protein and a Flavan-3-ol By NMR: Residual Structures in the Natively Unfolded Protein Provides Anchorage Points for the Ligands. *Biopolymers* **2009**, *91*, 745–756.
- (30) Pascal, C.; Poncet-Legrand, C.; Imbert, A.; Gautier, C.; Sarni-Manchado, P.; Cheynier, V.; Vernhet, A. Aggregation of a Proline-Rich Protein Induced by Epigallocatechin Gallate and Condensed Tannins: Effect of Protein Glycosylation. *J. Agric. Food Chem.* **2007**, *55*, 4895–4901.
- (31) Pramanik, B. N.; Bartner, P. L.; Mirza, U. A.; Liu, Y.-H.; Ganguly, A. K. Electrospray Ionization Mass Spectrometry for the Study of Non-Covalent Complexes: an Emerging Technology. *J. Mass Spectrom.* **1998**, *33*, 911–920.
- (32) Gabelica, V.; Rosu, F.; Houssier, C.; Pauw, E. D. Gas Phase Thermal Denaturation of an Oligonucleotide Duplex and its Complexes with Minor Groove Binders. *Rapid Commun. Mass Spectrom.* **2000**, *14*, 464.

- (33) Sarni-Manchado, P.; Cheynier, V. Study of Noncovalent Complexation between Catechin Derivatives and Peptide by Electro-spray Ionization-Mass Spectrometry (ESI-MS). *J. Mass Spectrom.* **2002**, *37*, 609–616.
- (34) Simon, C.; Barathieu, K.; Laguerre, M.; Schmitter, J. M.; Fouquet, E.; Pianet, I.; Dufourc, E. J. Three-Dimensional Structure and Dynamics of Wine Tannin-Saliva Protein Complexes. A Multi-technique Approach. *Biochemistry* **2003**, *42*, 10385–10395.
- (35) Canon, F.; Paté, F.; Meudec, E.; Marlin, T.; Cheynier, V.; Giuliani, A.; Sarni-Manchado, P. Characterization, Stoichiometry, and Stability of Salivary Protein-Tannin Complexes by ESI-MS and ESI MS/MS. *Anal. Bioanal. Chem.* **2009**, *395*, 2535–2545.
- (36) Canon, F.; Giuliani, A.; Pate, F.; Sarni-Manchado, P. Ability of a Salivary Intrinsically Unstructured Protein to Bind Different Tannin Targets Revealed by Mass Spectrometry. *Anal. Bioanal. Chem.* **2010**, *398*, 815–822.
- (37) Canon, F.; Ballivian, R.; Chirot, F.; Antoine, R.; Sarni-Manchado, P.; Lemoine, J.; Dugourd, P. Folding of a Salivary Intrinsically Unstructured Protein upon Binding to Tannins. *J. Am. Chem. Soc.* **2011**, *133*, 7847–7852.
- (38) Pascal, C.; Bigey, F.; Ratomahenina, R.; Boze, H.; Moulin, G.; Sarni-Manchado, P. Overexpression and Characterization of two Human Salivary Proline Rich Proteins. *Protein Expression Purif.* **2006**, *47*, 524–532.
- (39) Neyraud, E.; Heinzerling, C. I.; Bult, J. H. F.; Mesmin, C.; Dransfield, E. Effects of Different Tastants on Parotid Saliva Flow and Composition. *Chemosensory Perception* **2009**, *2*, 108–116.
- (40) Macakova, L.; Yakubov, G. E.; Plunkett, M. A.; Stokes, J. R. Influence of Ionic Strength on the Tribological Properties of Pre-Adsorbed Salivary Films. *Tribol. Int.* **2011**, *44*, 956–962.
- (41) Daniel, J. M.; Friess, S. D.; Rajagopalan, S.; Wendt, S.; Zenobi, R. Quantitative Determination of Noncovalent Binding Interactions using Soft Ionization Mass Spectrometry. *Int. J. Mass Spectrom.* **2002**, *216*, 1–27.
- (42) Greig, M. J.; Gaus, H.; Cummins, L. L.; Sasmor, H.; Griffey, R. H. Measurement of Macromolecular Binding Using Electrospray Mass Spectrometry. Determination of Dissociation Constants for Oligonucleotide: Serum Albumin Complexes. *J. Am. Chem. Soc.* **1995**, *117*, 10765.
- (43) Evans, D. F.; Wennerström, H. *The Colloidal Domain: Where Physics, Chemistry, Biology, and Technology Meet*; Wiley-VCH: New York, NY, 1994; eq 2.4.14
- (44) Poncet-Legrand, C.; Gautier, C.; Cheynier, V.; Imberty, A. Interactions between Flavan-3-ols And Poly(L-Proline) Studied by Isothermal Titration Calorimetry: Effect of the Tannin Structure. *J. Agric. Food Chem.* **2007**, *55*, 9235–9240.
- (45) Charlton, A. J.; Baxter, N. J.; Lokman Khan, M.; Moir, A. J. G.; Haslam, E.; Davies, A. P.; Williamson, M. P. Polyphenol/Peptide Binding and Precipitation. *J. Agric. Food Chem.* **2002**, *50*, 1593–1601.
- (46) Lannibois, H.; Hasmy, A.; Botet, R.; Aguerre Chariol, O.; Cabane, B. Surfactant limited aggregation of hydrophobic molecules in water. *J. Phys. II* **1997**, *7*, 319–342.
- (47) Golebiowski, J.; Fiorucci, S.; Adrian-Scotto, M.; Fernandez-Carmona, J.; Antonczak, S. Molecular Features Underlying the Perception of Astringency as Probed by Molecular Modeling. *Mol. Inf.* **2011**, *30*, 410–414.
- (48) Siebert, K. J.; Troukhanova, N. V.; Lynn, P. Y. Nature of Polyphenol-Protein Interactions. *J. Agric. Food Chem.* **1996**, *44*, 80–85.
- (49) Scharbert, S.; Holzmann, N.; Hofmann, T. Identification of the Astringent Taste Compounds in Black Tea Infusions by Combining Instrumental Analysis and Human Bioresponse. *J. Agric. Food Chem.* **2004**, *52*, 3498–3508.
- (50) Rinaldi, A.; Gambuti, A.; Moio, L. Precipitation of Salivary Proteins After the Interaction with Wine: The Effect of Ethanol, pH, Fructose, and Mannoproteins. *J. Food Sci.* **2012**, *77*, C485–C490.
- (51) Macakova, L.; Yakubov, G. E.; Plunkett, M. A.; Stokes, J. R. Influence of Ionic Strength Changes on the Structure of Pre-Adsorbed Salivary Films. A Response of a Natural Multi-Component Layer. *Colloids Surf, B* **2010**, *77*, 31–39.
- (52) Bradway, S. D.; Bergey, E. J.; Jones, P. C.; Levine, M. J. Oral Mucosal Pellicle. Adsorption and Transpeptidation of Salivary Components to Buccal Epithelial Cells. *Biochem. J.* **1989**, *261*, 887–896.
- (53) Soares, S.; Vitorino, R.; Osorio, H.; Fernandes, A.; Venancio, A.; Mateus, N.; Amado, F.; Freitas, V. D. Reactivity of Human Salivary Proteins Families Toward Food Polyphenols. *J. Agric. Food Chem.* **2011**, *59*, 5535–5547.